



ELSEVIER

Available online at www.sciencedirect.com

SCIENCE @ DIRECT®

Earth and Planetary Science Letters 219 (2004) 155–169

EPSL

www.elsevier.com/locate/epsl

Patterns of magma flow in segmented silicic dikes at Summer Coon volcano, Colorado: AMS and thin section analysis

Michael P. Poland^{a,*}, Jonathan H. Fink^a, Lisa Tauxe^b

^a Department of Geological Sciences, Arizona State University, Box 871404, Tempe, AZ 85282-1404, USA

^b Scripps Institution of Oceanography, La Jolla, CA 92093-0220, USA

Received 28 February 2003; received in revised form 10 November 2003; accepted 21 November 2003

Abstract

A complex pattern of magma flow is found in two silicic dikes of a radial swarm at Summer Coon, an eroded stratovolcano in southern Colorado. The two intrusions are broken into multiple segments that suggest vertical dike propagation. However, anisotropy of magnetic susceptibility (AMS) measurements and thin section observations suggest that magma flow was often subhorizontal and away from the center of the volcano. Segments that are proximal to the central intrusion are characterized by magma that flowed steeply upward at the proximal segment extremity, then laterally along the segment, and finally downward at the distal end of the segment. Magma flow in offset segment tips located far from the volcano center was subhorizontal towards the adjacent segment, implying lateral propagation of segment tips towards one another. This observation suggests relatively high driving pressure in distal dike segments, as supported by dike thickening with radial distance from the center of the volcano. The present study indicates that radial dike evolution at stratovolcanoes is dominated by lateral flow of magma and dike segmentation is a poor magma flow indicator. A horizontally propagating radial dike has the potential to cause an eruption low on the flank of a composite cone, which poses a significant yet largely unrecognized hazard to population centers and infrastructure that may surround the volcano.

Published by Elsevier B.V.

Keywords: anisotropy of magnetic susceptibility; magnetic fabric; radial dike intrusion; magma flow

1. Introduction

Dike intrusion is considered a common form of magmatism at composite volcanoes, even though the active process cannot be directly observed and

must be inferred from geophysical data or eroded sites. For example, deformation and seismicity in 1996 at Akutan volcano, Alaska has been attributed to the injection of a dike within 1 km of the surface [1]. Repeated dike intrusion may result in the development of a radial dike swarm, typified by the classic exposures of the Spanish Peaks in Colorado [2–6]. The orientation of individual dikes in the swarm reflects the stress field at the time of intrusion, and the swarm is manifested at the surface by a pattern of flank eruptive vents [7,8]. Determining whether such dikes intrude lat-

* Corresponding author. Present address: USGS - Cascades Volcano Observatory, 1300 SE Cardinal Ct., Suite 100, Vancouver, WA 98683-9589, USA. Tel.: +1-360-993-8957.

E-mail addresses: mpoland@usgs.gov (M.P. Poland), jon.fink@asu.edu (J.H. Fink), ltauxe@ucsd.edu (L. Tauxe).

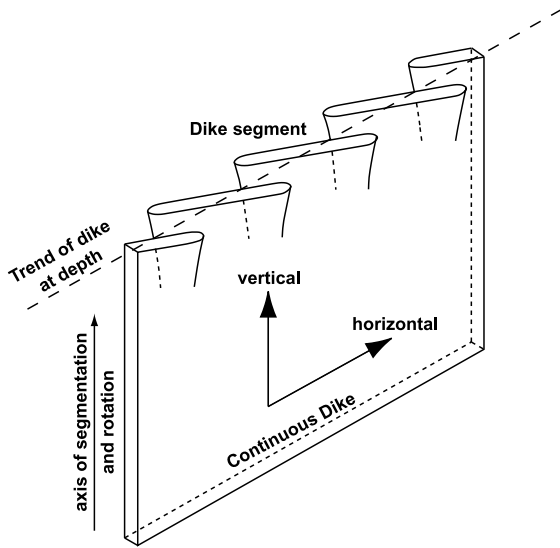


Fig. 1. Three-dimensional schematic view of a segmented, en echelon dike; modified from Delaney and Pollard [11].

erally, vertically, or obliquely is important for characterizing future eruptive behavior of the host volcano. If radial dikes form predominantly by the lateral flow of magma, eruptions have the potential to occur far from the magma source at the center of the volcano, which poses a greater hazard to surrounding population centers and infrastructure than an eruption from the upper flanks of the cone.

Existing evidence regarding dike propagation at shallow depths is contradictory. Flow directions have been inferred from the geometry of igneous fingers and segments that typify the margins of ancient intrusions and extend into the surrounding host rock [9,10] (Fig. 1). These offset segments are often arranged en echelon, slightly askew from the main dike trend [11]. However, the magma flow pattern within en echelon dike segments has been the subject of some debate [9,11–13]. Flow patterns in dike segments have been addressed by a few quantitative studies of structural lineations, mineralogical elongations and anisotropy of magnetic susceptibility (AMS) [6,14–17]. Often, however, the inferred flow direction for an entire dike is based on only one sample or measurement site (e.g., [18,19]), while the segmented geometry and connection to surface vents

implies complex magma flow in dikes. To resolve this expected complexity we collected samples for AMS and petrographic analysis from multiple locations along two silicic dikes of a radial swarm at the eroded Summer Coon volcano, Colorado. Both dikes are characterized by several sub-parallel, offset, rotated segments and were intruded within 3 km of the ground surface [20]. Our goal is to use AMS and thin section observations to characterize magma flow within a segmented dike. The results provide the most detailed example to date of how magma moves within a radial dike swarm and should be useful for hazards assessment during periods of unrest at active stratovolcanoes.

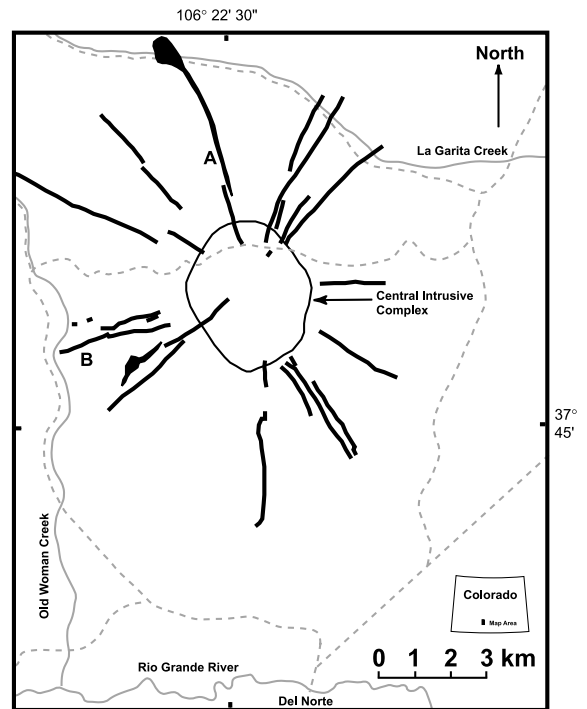


Fig. 2. Simplified map of Summer Coon volcano showing radial silicic dikes (heavy black solid lines). Basaltic andesite dikes are not shown; inset shows location in Colorado; gray solid lines are rivers and creeks; gray dashed lines are roads. Samples were collected for AMS analysis from Dikes A and B.

2. Summer Coon volcano

Summer Coon volcano is located approximately 10 km north of the town of Del Norte on the western edge of the San Luis Valley in south-central Colorado (Fig. 2). The volcano is part of the San Juan volcanic field, a region which covers 25 000 km² in southwestern Colorado and northern New Mexico and includes many silicic calderas and stratovolcanoes [21]. K–Ar and ⁴⁰Ar/³⁹Ar dates indicate that Summer Coon was active for 100 000–200 000 years between about 32 and 34 Ma [21,22]. Based on a paleotopographic reconstruction using a projected contact near the upper surface of the volcanic pile, Moats [20] determined minimum dimensions for Summer Coon of 4200 m elevation (2200 m above the basement), 110 km³ volume, and 17° average surface slope. Erosion has destroyed much of the original Summer Coon edifice, removing an estimated 59 km³ of material and decreasing the height of the volcano by 1700 m. Only parts of the central intrusive stocks, radial dikes, and some distal extrusive deposits are preserved [20,23,24].

Compositions ranging from basaltic andesite to rhyolite are represented in the intrusive and extrusive deposits of Summer Coon. The compositional development of the volcano can be divided into at least two episodes: (1) an early, voluminous, mafic phase dominated by basaltic andesite with minor amounts of rhyolite and dacite, and (2) a less voluminous, late stage phase of dacite magmatism [23–25]. Mafic compositions at Summer Coon were formed by partial melting of a garnet-bearing, trace element-enriched source, while silicic magma fractionally crystallized from the mafic parent.

The most distinguishing characteristic of Summer Coon is the pattern of radial dikes that emanates from its center (Fig. 2). The swarm consists of hundreds of basaltic andesite dikes that have short outcrop lengths (~200 m) and are poorly exposed [25], and about 20 large silicic dikes of dacite to rhyolite composition (Table 1). Exposed silicic intrusions can be up to 6.5 km long with cross-sectional widths of 1–50 m, multiple en echelon segments, and local relief that can exceed 20 m [20,23–25]. The lack of ero-

sional products and the presence of grooves and ridges that formed during intrusion imply that the dikes have not been substantially eroded (although the brittle, devitrified chill zones along the margins have been removed) and the current exposures are near the original upper surfaces of the intrusions. A curious anomaly common to nearly all silicic dikes at Summer Coon is an increase in thickness with radial distance [20]. If a dike is driven solely by overpressure in a magma reservoir, the viscous pressure drop along the length of the intrusion should cause the dike to thin with distance from the source [26]. An increase in thickness indicates higher driving pressures (defined as the difference between magma pressure and the least compressive stress in the crust [27]) with radial distance, perhaps due to shallowing burial depths under the sloping flanks of the volcano, a gradient in the regional stress field, or changing host rock properties [26]. The fact that neither the mafic nor silicic dikes deviate significantly from radial orientations suggests that the regional state of horizontal stress was nearly isotropic at the time of intrusion. The entire volcanic pile has an asymmetric dip and appears to have been tilted approximately 7° to the southeast [20], but the regional tilting occurred at least 5 Myr after the cessation of activity at Summer Coon and was probably related to the formation

Table 1
Characteristics of sampled dikes

	Dike A	Dike B
SiO ₂	61.59	67.20
Al ₂ O ₃	15.36	14.93
Fe ₂ O ₃	1.89	2.09
FeO	3.08	0.40
MnO	0.08	0.03
MgO	2.63	0.83
CaO	3.75	2.00
TiO ₂	0.63	0.50
Na ₂ O	4.34	4.26
K ₂ O	3.55	4.17
H ₂ O	1.61	1.63
CIPW Mt (%)	2.74	0.23
Density (g/cm ³)	2.48	2.47

Chemical compositions and magnetite weight percents from CIPW were published by [24, plates 1 and 2], and densities of samples from Dikes A and B were determined from the core samples.

of the Rio Grande Rift to the east at about 25 Ma. Thus, a regional stress gradient is probably not the cause of the inferred increase in dike driving pressure with radial distance, which is more likely to be a result of some combination of shallowing burial depths and changing host rock properties.

3. Magnetic analysis

3.1. Background

Macroscopic indicators of magma flow, including grooves, slickensides, and aligned vesicles, are rare in Summer Coon dikes. Therefore, we used AMS measurements and thin section observations of aligned phenocrysts to map flow patterns. AMS determines the internal rock fabric based on the alignment of magnetically ‘easy’, or susceptible, directions in iron-rich minerals [28,29]. In igneous rocks, this shape-preferred orientation is generally attributed to magma flow [30,31]. The two main contributors to AMS are paramagnetic (iron-bearing) elongated minerals, such as biotite, and more importantly ferromagnetic crystals, usually titanomagnetites. Paramagnetic minerals usually have axes of magnetic susceptibility that correspond to their crystallographic axes (short axis is less magnetically susceptible), thus flow-aligned biotite crystals, for example, are expected to have a magnetic anisotropy fabric that is coaxial with the flow fabric [31,32]. Titanomagnetite grains are generally small and spherical, and often crystallize late in the cooling history after flow has ceased. The distribution of titanomagnetite clusters can simulate an elongated mineral grain as the fill between the existing flow-induced fabric. This ‘distribution anisotropy’ is cited as the primary source of AMS in most igneous rocks [31,33].

Flow directions in dikes can be constrained with AMS by collecting samples from opposing margins of an intrusion [18]. Simple shear caused by flow along unmoving wall rock will cause rotation of elongated tabular phenocrysts (e.g., plagioclase and biotite), which collide and become stacked or imbricated against one another [18, 30]. As a result, the long crystallographic axes of

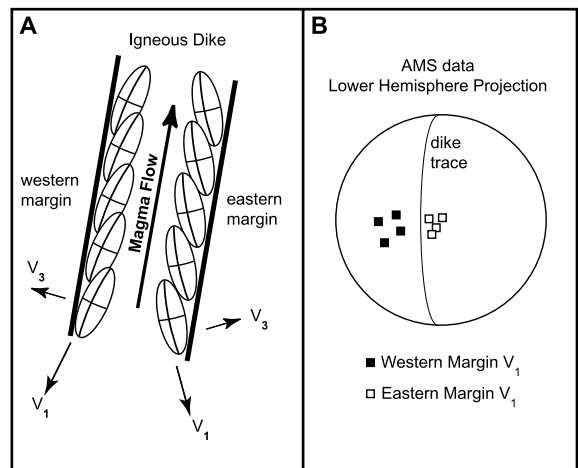


Fig. 3. (A) A conceptual model for the behavior of elongated phenocrysts and clusters of small magnetite grains in a dike, shown schematically in vertical section. The magma flow in the dike is expected to rotate the elongated crystals into a parallel, stacked geometry, plunging in the direction of flow and oblique to the dike wall. (B) The expected V_1 directions for the eastern and western margins of the dike, indicated in A, plot east and west of the dike trace respectively, indicating subvertical flow of magma. Modified from Tauxe ([29], p. 236).

the mineral grains are likely to be oriented at a small angle with respect to the dike margin, plunging towards the magma source (Fig. 3). The axis of maximum susceptibility (V_1) for iron-bearing minerals and clusters of titanomagnetite grains that crystallize in this matrix will parallel the direction of the long axes, while the minimum susceptibility (V_3) will be at a small angle from the normal to the dike margins. The axis of intermediate susceptibility (V_2) should be perpendicular to both V_1 and V_3 and contained within the dike plane [18,29,31,32,34]. Assuming that a dike is emplaced in an extensional fracture (i.e., no wall-parallel shear occurs during magma injection), samples from opposing dike margins should show V_1 directions that are imbricated in contradictory directions, enabling a unique flow direction to be inferred [18,35] (Fig. 3). Dikes that experience shearing during emplacement, perhaps due to intrusion into a transform fault, will have an asymmetric distribution of imbricated phenocrysts on opposing margins [35,36]. No evidence exists to indicate that Summer Coon dikes

Table 2
AMS data and statistics

Sample site	N	Dike attitude		κ (μSI)	Maximum susceptibility				Intermediate susceptibility				Minimum susceptibility				Ani. (%)	Flow vectors	Field data
		Dip	Direction		τ_1	σ	Dec	Inc	τ_2	σ	Dec	Inc	τ_3	σ	Dec	Inc			
A-1	9	88	064	17941	0.33665	0.00040	2.0	35.5	0.33414	0.00028	157.1	51.8	0.32921	0.00022	263.1	12.2	0.74	lineation only	
A-2	8	88	064	25026	0.33576	0.00014	327.3	6.2	0.33394	0.00017	75.7	71.0	0.33029	0.00013	235.3	17.9	0.55	lineation only	
A-3	5	88	064	21120	0.33782	0.00033	358.7	71.6	0.33411	0.00059	181.8	18.4	0.32807	0.00030	91.5	0.9	0.98	lineation only	
A-4	5	88	064	26449	0.33839	0.00023	336.2	0.3	0.33421	0.00021	69.4	84.9	0.32739	0.00023	246.1	5.1	1.10	lineation only	
A-5	5	88	064	19111	0.33603	0.00011	358.4	3.3	0.33406	0.00016	113.3	82.1	0.32991	0.00011	268.0	7.1	0.61	N3 \pm 11	
A-6	5	83	071	23321	0.33579	0.00098	151.7	41.6	0.33470	0.00079	350.8	46.8	0.32951	0.00163	250.4	9.6	0.63	lineation only	
A-7	6	83	071	19032	0.33605	0.00029	130.7	12.3	0.33368	0.00030	305.2	77.6	0.33027	0.00029	40.5	1.2	0.58	S–11 \pm 16	
A-8	9	83	071	23255	0.33824	0.00027	172.4	68.0	0.33349	0.00064	352.7	22.0	0.32827	0.00059	262.7	0.1	1.00	N63.5 \pm 12.5	N72
A-9	3	83	074	31302	0.34182	0.00020	1.3	40.2	0.33626	0.00045	202.6	47.8	0.32192	0.00051	100.5	10.8	1.99	ND	
A-10a	3	86	140	29291	0.33714	0.00061	194.4	57.6	0.33442	0.00035	14.6	32.4	0.32844	0.00027	284.5	0.1	0.87	N59 \pm 11	
A-10b	3	86	062	25126	0.34034	0.00018	45.1	63.6	0.33448	0.00007	190.0	22.1	0.32517	0.00019	285.7	13.7	1.52	S84.5 \pm 5.5	
A-11	5	88	064	27925	0.33797	0.00068	317.0	5.1	0.33399	0.00032	196.7	80.0	0.32804	0.00062	47.8	8.6	0.99	N1.5 \pm 11.5	
A-12	5	85	060	26405	0.33673	0.00020	124.5	44.3	0.33402	0.00052	340.3	39.7	0.32925	0.00037	233.9	18.8	0.75	N47 \pm 14	N70
A-13	5	85	060	27068	0.33810	0.00039	185.3	54.9	0.33376	0.00066	321.3	26.8	0.32813	0.00048	62.4	20.9	1.00	N59.5 \pm 20.5	N64
A-14	6	78	270	25773	0.33906	0.00037	355.3	32.4	0.33366	0.00061	236.3	37.3	0.32727	0.00094	112.7	36.0	1.18	S32 \pm 7	S–45
B-1	5	75	349	25068	0.33779	0.00044	111.2	61.2	0.33512	0.00014	240.5	19.2	0.32709	0.00042	338.1	20.6	1.07	W61 \pm 5	
B-2	3	84	349	20756	0.33618	0.00023	286.8	60.2	0.33459	0.00026	59.5	21.2	0.32923	0.00012	157.6	19.9	0.69	ND	
B-3	6	88	341	15106	0.33707	0.00011	190.7	67.9	0.33341	0.00025	55.9	16.0	0.32952	0.00023	321.5	14.9	0.76	W75 \pm 7	
B-4	5	84	335	11473	0.33781	0.00020	58.0	17.1	0.33400	0.00026	280.4	67.4	0.32818	0.00021	152.5	14.3	0.96	W16 \pm 3	
B-5	4	84	335	10788	0.33600	0.00016	71.7	14.3	0.33413	0.00023	206.9	70.2	0.32988	0.00015	338.2	13.4	0.61	W7 \pm 12	W18
B-6	7	87	340	9379	0.33573	0.00053	243.7	6.0	0.33247	0.00043	9.5	79.8	0.33180	0.00056	152.8	8.2	0.39	W–12 \pm 16	
B-7	5	87	340	12500	0.33677	0.00010	270.9	5.5	0.33367	0.00017	152.0	78.7	0.32955	0.00019	1.8	9.8	0.72	W–8 \pm 15	
B-8	3	80	000	21225	0.33825	0.00012	174.7	76.4	0.33237	0.00013	46.9	8.5	0.32938	0.00023	315.3	10.6	0.89	W88 \pm 4	
B-9	5	85	351	15424	0.33610	0.00014	287.2	29.5	0.33381	0.00021	78.7	57.3	0.33009	0.00026	189.7	13.0	0.60	W–33 \pm 7	
B-10	5	80	342	13521	0.33803	0.00012	43.4	57.3	0.33388	0.00026	241.3	31.4	0.32808	0.00026	146.3	8.1	1.00	W61.5 \pm 6.5	
B-11	5	86	170	14021	0.33733	0.00019	69.1	67.7	0.33319	0.00013	261.0	21.9	0.32948	0.00009	169.4	4.2	0.79	W68.5 \pm 3.5	
B-12	3	86	170	20976	0.33758	0.00028	109.7	59.2	0.33308	0.00021	245.3	23.1	0.32935	0.00011	343.9	19.2	0.82	W64 \pm 4	
B-13	4	83	337	4450	0.33512	0.00028	38.4	0.0	0.33363	0.00017	308.4	63.5	0.33125	0.00024	128.5	26.5	0.39	E7 \pm 12	
B-14	5	83	316	6113	0.33585	0.00017	202.0	7.3	0.33348	0.00020	9.2	82.6	0.33066	0.00035	111.8	1.6	0.52	E6 \pm 12	
B-15	5	83	316	15156	0.33652	0.00045	206.0	8.3	0.33354	0.00018	312.8	63.2	0.32994	0.00032	112.0	25.3	0.66	E14 \pm 17	
B-16	4	75	006	12049	0.33708	0.00010	274.8	24.7	0.33382	0.00016	37.4	49.5	0.32910	0.00011	169.5	29.8	0.80	W–22.5 \pm 4.5	
B-17	5	89	349	5401	0.33500	0.00027	19.0	67.4	0.33355	0.00019	237.0	18.1	0.33144	0.00024	142.7	13.0	0.36	W82 \pm 13	
B-18	4	89	349	1183	0.33526	0.00036	136.2	64.4	0.33452	0.00038	287.0	22.7	0.33022	0.00063	21.8	11.2	0.50	W51.5 \pm 14	

Magnitude and orientation for the maximum (τ_1), intermediate (τ_2) and minimum (τ_3) susceptibilities for each site are listed along with the standard deviation (σ), anisotropy percent (Ani. %, as defined by [40]), number of samples (N), local dike attitude (given as dip and dip direction), and bulk susceptibility (κ). Ani. % and κ are reported as averages of all samples at a site. Flow vectors from AMS are given as direction and degrees from horizontal (e.g., N–11 \pm 16 means flow to the north, down 11 \pm 16 degrees from the horizontal). ND=no flow direction determined because τ_1 and τ_2 are not distinct at the 95% confidence level. Field data refer to macroscopic flow lineations observed at Summer Coon, for example, grooves in dike margins or aligned vesicles or phenocrysts, and follow the same convention as the flow vectors.

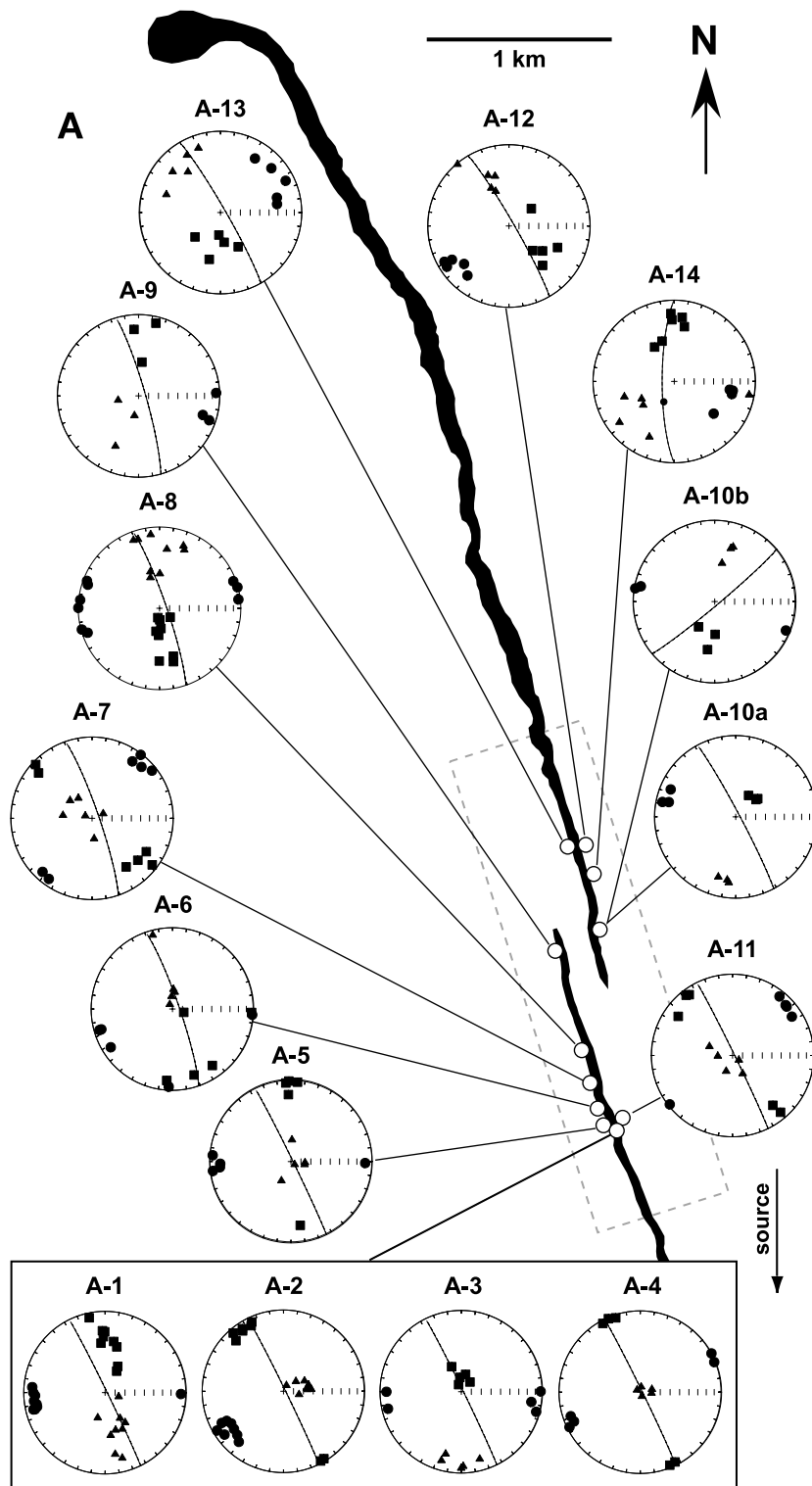


Fig. 4.

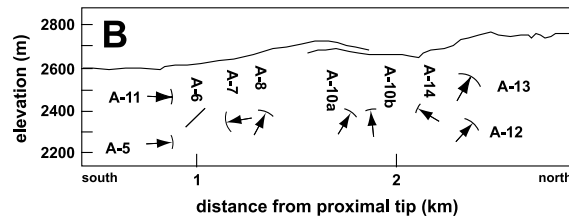


Fig. 4 (Continued). Flow directions inferred from AMS data along Dike A at Summer Coon volcano. (A) Map view showing sample sites (white dots), AMS data in lower hemisphere stereographic projections (squares = maximum axis of magnetic susceptibility, triangles = intermediate axis of magnetic susceptibility, circles = minimum axis of magnetic susceptibility), and area of cross-section shown in B (outlined by gray dashed box). (B) Cross-section showing magma flow directions as arrows with 95% confidence arcs at the arrow tips (a lineation only was determined at site A-6). The elevation of the exposed dike top is plotted versus distance from the dike end that is proximal to the central intrusive complex (see Fig. 2).

occupy shear fractures and the near perfect radial form of the dike swarm suggests a nearly isotropic stress field. Further, the AMS results described below are symmetrical about opposing margins, so we infer that the dikes occupy extensional fractures.

3.2. Sampling and magnetic characterization

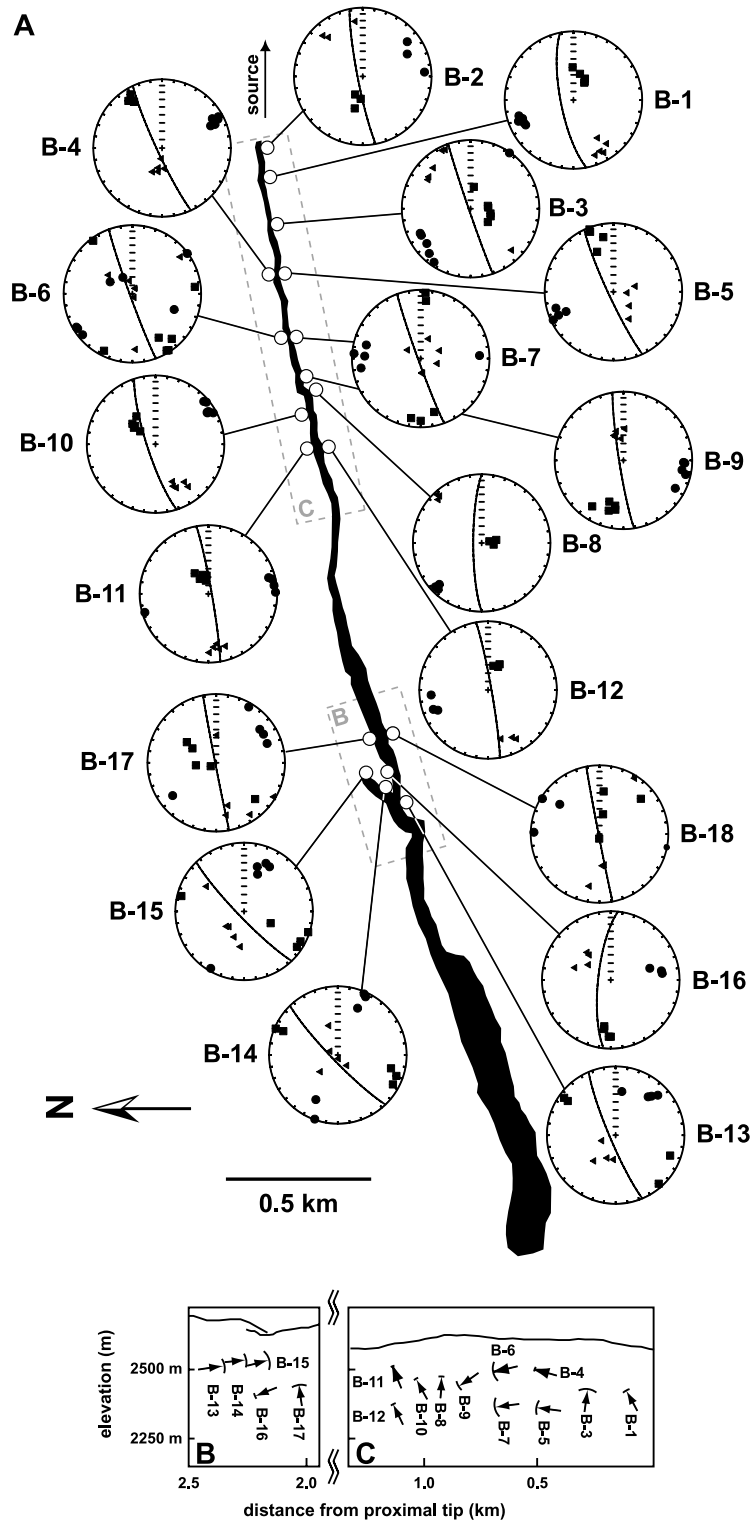
Our sampling procedure follows Tauxe ([29], pp. 237–239). All samples were drilled in situ using a portable drill and oriented using a magnetic compass (a sun compass was not necessary due to the low magnetization of the dikes). Samples were taken from the dike margins (except where noted) to ensure that the measured magma flow direction reflects the initial intrusion of the dike according to the simple shear process shown in Fig. 3. At least five 24 mm diameter drill cores were obtained from each site, although orienting uncertainties and post-sampling damage made some cores unusable (which is why some sites have fewer than five AMS data points). The cores were cut into sections of 24 mm length, with each core yielding one to three specimens.

Dike A, extending 6.5 km north from the center of the volcano (Figs. 2 and 4A), was sampled at 15 sites over its southern portion, which includes an en echelon separation of ~ 150 m. To assess magma flow directions within the inner core of the dike, samples from sites A-1–4 were collected along a cross-section perpendicular to the dike (Fig. 4A). Dike B, which stretches west from the

center of Summer Coon (Fig. 2), was sampled at 18 locations over two offset segments (Fig. 5A).

A total of 165 specimens from 33 sites were used in the AMS analysis. Magnetic susceptibility was measured with a KLY-2 Kappabridge susceptibility meter. Bulk susceptibilities (for sites averaged from samples) ranged from 10^{-3} to 3×10^{-2} SI with a mean of 1.8×10^{-2} SI (Table 2), and are generally higher for Dike A, which has a greater weight percent magnetite (Table 1). From Rochette et al. [32] and the chemical compositions of the dikes (Table 1, after [24], plates 1 and 2), we calculated the contribution of paramagnetic minerals to the measured susceptibilities of Dikes A and B to be 251 μ SI and 129 μ SI, respectively. The values are one to several orders of magnitude less than measured, suggesting that ferromagnetic minerals are the dominant cause of AMS in Summer Coon dikes.

Curie temperature measurements identify titanomagnetite as the primary magnetic mineral (Fig. 6A), which is supported by calculated magnetite weight percents of 2.74% (Dike A) and 0.23% (Dike B) [24]. Hysteresis loops measured on an alternating gradient force magnetometer indicate that the magnetic minerals responsible for the AMS signal are multi-domain (Fig. 6B), which is preferable for AMS studies [34]. The presence of single-domain magnetic minerals often leads to ‘inverse’ AMS fabrics that are perpendicular to the true magma flow direction [37]. However, samples from Summer Coon are multi-domain and ferromagnetic, suggesting that the



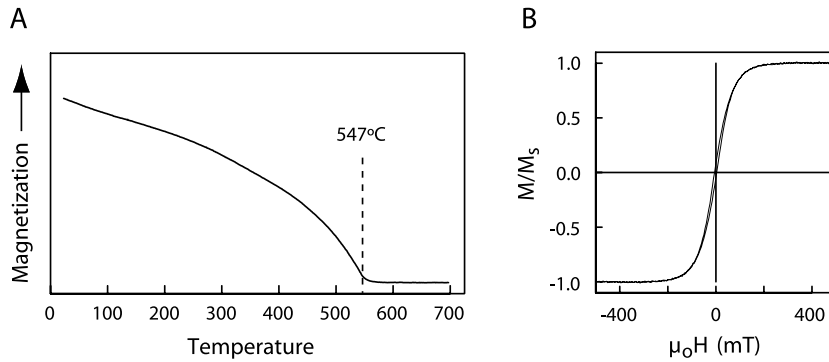


Fig. 6. (A) Curie temperature measurement of sample 3-2E; here and in most other samples the Curie temperature is approximately 550°C, suggesting titanomagnetite as the primary magnetic mineral. (B) Hysteresis loop from sample 8-5E. The sample is typical of all those that were measured, and implies the presence of a multi-domain magnetic carrier. The vertical axis is the induced magnetization (M) normalized by the saturation magnetization (M_s), and the horizontal axis is the applied field (H) times the permeability of free space (μ_0), in units of milliTesla (mT).

measured AMS fabric is an accurate indicator of magma flow in the sampled dikes. The magnetic characteristics of dikes at Summer Coon are similar to those described by Aubourg et al. [38], who analyzed rhyolite dikes in Italy and found ferromagnetic susceptibilities (10^{-4} – 10^{-2} SI) and Curie temperatures of 580°C.

3.3. AMS results

We assess the quality of the AMS data using the statistical bootstrap for dikes of Tauxe et al. [34]. Of the 33 sites sampled (Table 2), none yielded ‘inverse’ fabrics (as defined by [39]), which is consistent with AMS measurements of other rhyolite dikes [38]. Studies of basaltic dikes, in contrast, generally find some proportion of inverse fabrics [18,34,37]. ‘Normal’ fabrics are defined by V_1 at a small angle to the dike plane, V_2 contained within the dike plane, and V_3 at a small angle to the dike margin. Some sites at Summer Coon are characterized by V_2 orientations that are not within the plane of the dike (for example, site B-8, Fig. 5A), but these discrepancies are likely caused by errors in the attitude measurement of the dikes, which can locally be quite com-

plex. The anisotropy of individual sites varies between 0.36% and 1.99% (Table 2), using the method of Tauxe et al. [40] where the percent anisotropy is defined as $100(\tau_1 - \tau_3)$, and τ_1 , τ_2 , and τ_3 are the magnitudes of the maximum, intermediate, and minimum susceptibilities, respectively (normalized such that $\tau_1 + \tau_2 + \tau_3 = 1$).

Knight and Walker [18] and Tauxe et al. [34] advocate sampling on both margins of a dike to confirm the flow direction because the long axes of the susceptibility ellipses determined from each margin should fall off the plane of the dike by the same amount but in opposite directions (Fig. 3), assuming the dike was emplaced within an extensional fracture [35,36]. Due to the difficulty in accessing many of the dike outcrops at Summer Coon, opposing margins were sampled at only six localities (12 sites out of the total 33). All of these areas satisfied the criteria of Tauxe et al. [34] for determining a unique flow direction (Fig. 7). Based on the success at the six localities, we treat sites with samples from one dike margin as indicating a unique flow direction when the long axis of the susceptibility ellipse was distinct from the dike plane at the 95% confidence level. Absolute magma flow directions can be inferred at 26 sites

←

Fig. 5. Flow directions from AMS data along Dike B at Summer Coon in map view (A) and cross-section (B,C). See Fig. 4 for an explanation of plotting conventions and symbols.

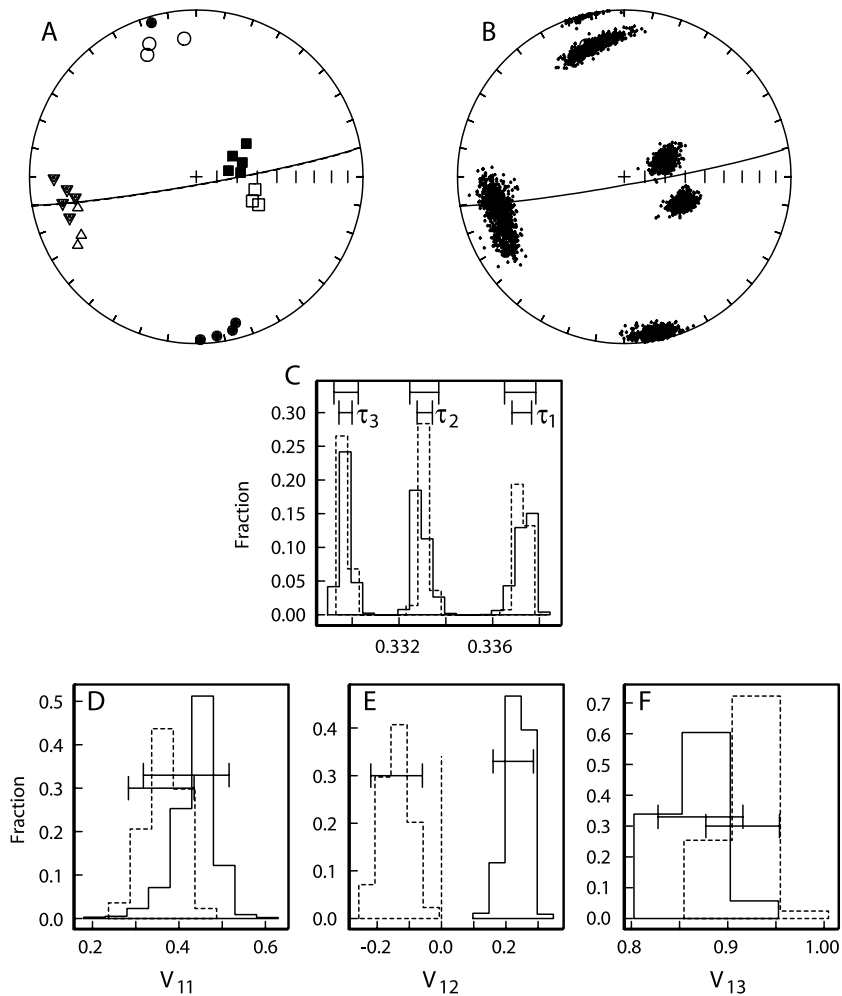


Fig. 7. The AMS dataset from sites B-11 (closed symbols, dashed histogram populations and bottom confidence values in C, D, and F) and B-12 (open symbols, solid histogram populations, and top confidence values in parts C, D, and F). (A) Lower hemisphere equal area projections showing eigenvector directions of individual specimens and the dike attitude (great circle). V_1 (squares), V_2 (triangles) and V_3 (circles) are shown for both sample sites. (B) Maximum, intermediate, and minimum eigenvectors of 1000 para-data sets (500 per site) from the data in A. (C) Histograms of the bootstrapped eigenvalues (τ_1 , τ_2 , and τ_3) for the two sites. Note that all three axes for each site are distinct at the 95% confidence level, which is required for identification of a unique flow direction. (D–F) Histograms of the cartesian coordinates of the bootstrapped eigenvectors rotated into dike coordinates. The dashed vertical line at $V_{12} = 0.0$ is the dike plane. A second requirement for determination of a unique flow direction is that 95% confidence values for each site are distinct from both each other and the dike plane. Note that both sites plot off the dike plane in opposite directions. Following the model shown in Fig. 3, magma flow is to the west and inclined approximately 65° upward from horizontal (flow inclination is determined from the arcsin of V_{13}) in this example.

using the aforementioned criteria. Four sites collected from the inner core of Dike A (sites A-1–4) only indicate flow lineations since samples were not taken from the dike margin, and a lineation can only be inferred from site A-6 because V_1

cannot be distinguished from the plane of the dike at the 95% confidence level. Neither directions nor lineations can be recovered from sites A-9 and B-2 because τ_1 and τ_2 cannot be distinguished at the 95% confidence level.

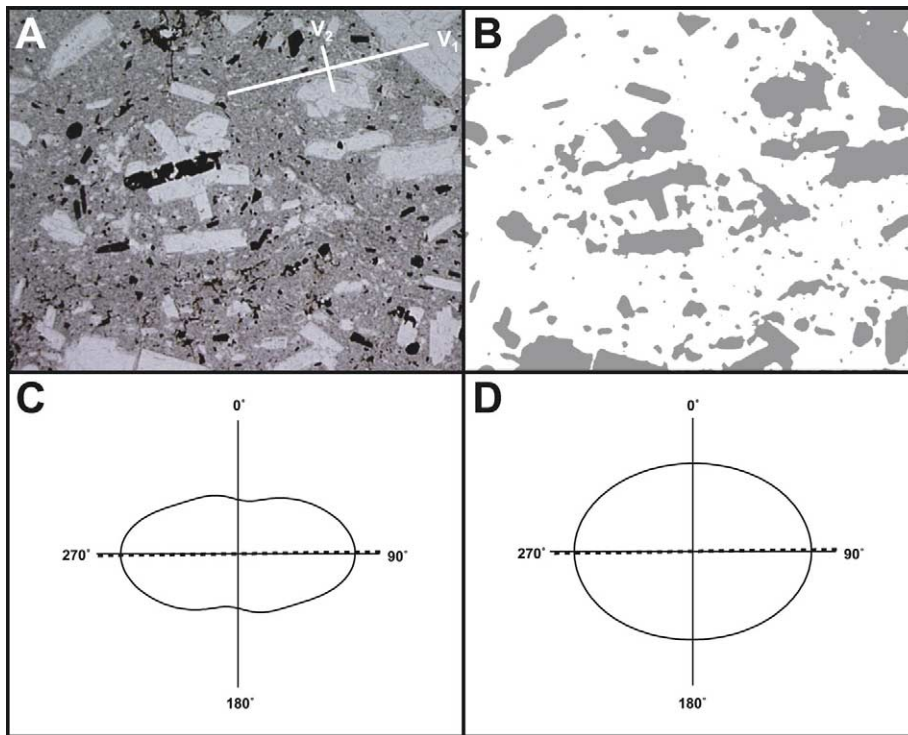


Fig. 8. Example of plagioclase petrofabric analysis taken from sample B-15C. (A) Plane-polarized light photomicrograph, field of view is approximately 10 mm. Flow lineation from AMS for site B-15 is shown in the upper left (error on V_1 is $\pm 14^\circ$). (B) Classified thin section, with plagioclase in gray and all other minerals and matrix in white. (C) Rose of directions for plagioclase boundary orientations, indicating 89.2° as the average plagioclase grain orientation. (D) Equivalent shape for plagioclase in the thin section.

4. Thin section analyses

When taken alone, the significance of the V_1 magnetic lineation is suspect. Other processes, such as crenulation of the magnetic foliation, can result in an alignment of V_1 axes that does not reflect the true magma flow direction [10,38]. In some cases, it appears that V_2 may represent the true flow direction [10,41,42]. As a result, it is important to confirm the AMS results with an independent measurement of magma flow (e.g., [10,15,38,43–45]). Macroscopic structural lineations along the dike margins are one such indicator. Grooves, slickensides, and similar features were observed at five of the 33 sample sites. At four of the locations, the measured lineations lie within 25° of the V_1 direction determined from AMS (Table 2).

We also compared the alignment of plagioclase

grains in thin section to the V_1 direction from AMS. Plagioclase orientation was used as a proxy for magma flow direction at the radial dike swarm of Lyttleton volcano, New Zealand [16,46]. We cut 102 oriented thin sections along the magnetic foliation plane (V_1 – V_2), which contains the AMS-derived flow direction. Digital photomicrographs (Fig. 8A) of the sections were then classified following Launeau et al. [47] to separate plagioclase, the dominant phase in all Summer Coon dikes, from the matrix and other mineral grains (Fig. 8B). Each photomicrograph was filtered to reduce the noise associated with the classification and processed with the INTERCEPT software [48], which uses a Fourier analysis to determine the boundary orientations of a specific phase. A circular window was chosen to minimize edge effects and the angular counting interval was set to 2° . The program output was entered into the

ROSES.XLS spreadsheet [48] to obtain a rose of directions and characteristic shape for each sample (Fig. 8C,D). For 68% of the sections analyzed, the preferred plagioclase orientation was within 30° of the AMS-derived V_1 direction. This result is comparable to that of Callot et al. [44], who found that plagioclase alignment and AMS fabric agreed in 66% of sampled dikes in East Greenland. Amphibole orientations from the INTERCEPT program in two of three thin sections of Dike A were also sub-parallel to the V_1 and plagioclase orientations for the same sections. The agreement between the plagioclase/amphibole orientations, macroscopic structural lineations, and magnetic anisotropy directions suggests that the magnetic fabric is flow-related. Further, V_1 appears to represent the actual flow direction, instead of V_2 , which has been suggested for some basaltic dikes in Iceland [41,42].

5. Discussion

The magnetic and thin section data generally show consistent patterns that allow magma flow in two dikes at Summer Coon volcano to be inferred. The flow profile of Dike A (Fig. 4B) suggests subhorizontal movement of magma within the interior of the southern segment (sites A-5, 7 and 11) with steeply inclined flow at the northern segment proximal to the center of the volcano (sites A-10 and 12–14). At sites A-7 and A-14, magma flow was toward the central intrusive complex at Summer Coon, the presumed source. This anomalous flow direction is probably real as the dike is well exposed, its attitude is well determined at both sites, and we found no irregularities in the magnetic fabric. Similar anomalous flow patterns over small length scales were observed in dikes of Makhtesh Ramon, Israel [14,49]. In general however, no such flow pattern is expected in a radial dike proximal to its pressurized source. For example, Shelley [16] found no evidence for lateral flow towards the source of the basalt to trachyte radial dike swarm at the analogous Lytleton volcano in New Zealand.

Samples were also collected along a section perpendicular to the margin of Dike A (sites A-1–4)

to examine the pattern of magma flow in the dike interior (Fig. 4A). Sites A-5 and A-11 from the western and eastern margins of the dike, respectively, indicate subhorizontal flow to the north at the location of the sampled section. However, magma flow in sites A-1–4, between sites A-5 and 11, varies widely and includes oblique (A-1), lateral (A-2 and A-4), and vertical (A-3) flow lineations (absolute directions cannot be determined because the samples were not collected at the dike margin). This variable flow pattern across the width of the dike may be a result of magma drain-back following an eruption, multiple intrusive phases, or other local effects [11,15,16,50]. Regardless, the measurements support our assumption that only magma flow measured along dike margins is an accurate representation of conditions at the time of initial dike emplacement.

The measured magma flow directions in the proximal segment of Dike B (sites B-1–7 and 9) suggest that magma entered an offset fracture from below and to the east and flowed west until reaching the western limit of the dike segment. The magma then flowed down and to the west (Fig. 5B). A similar pattern is apparent in the dike segment that begins at site B-8, which is also characterized by steeply inclined flow at its proximal extremity. In contrast, samples from segment tips of the distal offset of Dike B, near sites B-13–18, indicate magma flow in opposing segment tips towards each other. At this location, the geometry of the segments in map view strongly resembles that predicted by Olson and Pollard [51] for mechanically interacting echelon cracks, suggesting that flow in the dike tips may be in the direction of dike propagation. Magma flow towards dike segment tips was also found at Makhtesh Ramon, Israel [15], although the pattern occurs only within a few meters of the tips.

Baer [15] proposes that magma flow towards the tips of overlapping dike segments is related to the proximity of the tips. While this certainly seems to be the case in Dike B at sites B-13–18, magma flow in overlapping segments near sites A-9 and 10 of Dike A is not towards the tips (Fig. 5). This may be a result of the great distance between the overlapping segments (150 m). There is also a slight overlap between offset segments in

Dike B near sites B-8 and 9, with magma flow that is not towards the tips (at least in one segment). Here, however, the overlap is short, the dike is thin, and the driving pressure (inferred from dike thickness) was relatively low, so it seems likely that magma was not able to flow towards the dike tips before freezing against the margins. As stated previously, dikes at Summer Coon tend to thicken with distance from the center of the volcano, suggesting a corresponding increase in dike driving pressure [26]. Close to the center of the volcano, the driving pressure may be too low to cause magma to flow into segment tips along the dike margins, whereas the higher driving pressure far from the center of the volcano might result in flow that approximates the propagation direction of the dike.

The lack of a significant component of vertical flow in the middle of individual segments of Dikes A and B implies that the intrusions are not vertically extensive, but formed primarily due to lateral flow in a continuous dike that exists below the current exposure (Fig. 9). Isolated areas of steeply inclined flow occur along the upper surfaces of the dikes, which based on the lack of erosional products we infer to be currently exposed at Summer Coon. Magma from the continuous intrusion flowed up and into offset fractures, forming distinct segments. The fractures are either preexisting structures or, more likely, form due to concentrations of tensile stress that occur in front of and to the sides of a pressurized dike [52]. Poorly developed, minor segmentation does not appear to have an influence on the overall pattern of magma flow (location 1 in Fig. 9). However, when dike driving pressure is high (far from the center of the volcano where the dikes are thicker), and offset segments overlap and mechanically interact, mag-

ma flow is in the direction of the segment tips (location 2 in Fig. 9).

Results from Summer Coon suggest that magma flow in radial dikes at stratovolcanoes is generally subhorizontal, with locally steep flow vectors caused by irregularities in dike geometry (principally offset segments). The identification of horizontal magma flow in a dike that is segmented in horizontal section is an important result, since many models of dike intrusion use such segmentation as an indicator of vertical magma flow and dike propagation. Future studies of ancient dikes exposed by erosion should be careful not to infer magma flow based on dike geometry alone. Further, if magma flow in radial dike swarms is dominantly lateral, as suggested by observations from Summer Coon, a radial intrusion at a stratovolcano should be able to propagate several kilometers from its source. If such a dike reached the surface, an eruption could occur on the low flank of the edifice where population centers and infrastructure are most likely to be located. As a result, monitoring networks (especially geodetic) at active composite cones should be designed to recognize radial dike intrusions that may lead to eruptions far from the summit of the volcano.

6. Conclusions

Data from the present study suggest that AMS in silicic intrusions is a useful indicator of magma flow direction, especially when supported by thin sections and, where available, field evidence. Our AMS and thin section results from Summer Coon volcano imply that magma flow in segmented dikes is not necessarily parallel to the axis of segment rotation (Fig. 9). Consequently dike geometry may not be a reliable indicator of magma flow direction, as proposed previously [9,11–13]. Field studies of dikes exposed by erosion should avoid using offset segments as an indicator of magma flow direction without additional supporting evidence. The AMS and thin section data also indicate that the upper part of a dike commonly breaks into segments as magma from the continuous intrusion at depth flows into and dilates

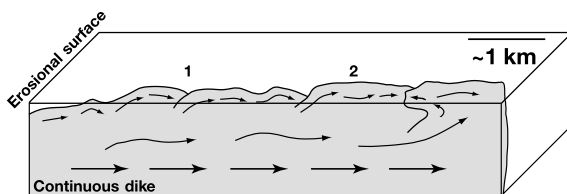


Fig. 9. Synthesis of magma flow in the silicic radial dikes at Summer Coon volcano. Locations 1 and 2 are discussed in the text.

fractures offset from the main dike trend. Where the dike driving pressure is high and segment ends overlap, flow can be towards the tips of the segments, perhaps mirroring the dike propagation direction. Further, abundant evidence for subhorizontal magma flow at Summer Coon suggests that silicic radial dikes have the potential to travel several kilometers from their sources, possibly resulting in eruptions far from the summit of the host volcano.

Acknowledgements

This work is part of M.P.P.'s doctoral dissertation at Arizona State University, which was supported by a National Defense Science and Engineering Graduate Fellowship. Fieldwork was funded by graduate research grants from the Geological Society of America, SCION Natural Science Association, and Colorado Scientific Society. John Geismann and Kenneth Verosub provided paleomagnetic sampling equipment, and Aaron Lyman and Chantelle Lucas assisted with fieldwork. Daniel Dzurisin, Cynthia Gardner, William Moats, Willie Scott, Sven Morgan, Keith Benn, Charlie Aubourg, and Ze'ev Reches provided constructive reviews. [VC]

References

- [1] Z. Lu, C. Wicks Jr., J.A. Power, D. Dzurisin, Ground deformation associated with the March 1996 earthquake swarm at Akutan volcano, Alaska, revealed by satellite radar interferometry, *J. Geophys. Res.* 105 (2000) 21483–21495.
- [2] H. Ode, Mechanical analysis of the dike pattern of the Spanish Peaks area, Colorado, *Geol. Soc. Am. Bull.* 68 (1957) 567–576.
- [3] O.H. Muller, Changing stresses during emplacement of the radial dike swarm at Spanish Peaks, Colorado, *Geology* 14 (1986) 157–159.
- [4] O.H. Muller, D.D. Pollard, The stress state near Spanish Peaks, Colorado, determined from a dike pattern, *Pure Appl. Geophys.* 115 (1977) 69–86.
- [5] R.B. Johnson, Patterns and origin of radial dike swarms associated with West Spanish Peak and Dike Mountain, south-central Colorado, *Geol. Soc. Am. Bull.* 72 (1961) 579–590.
- [6] R.P. Smith, Dyke emplacement at Spanish Peaks, Colorado, in: H.C. Halls, W.F. Fahrig (Eds.), *Mafic Dyke Swarms*, *Geol. Soc. Can. Spec. Pap.* 34 (1987) 47–54.
- [7] K. Nakamura, Volcanoes as possible indicators of tectonic stress orientation; Principle and proposal, *J. Volcanol. Geotherm. Res.* 2 (1977) 1–16.
- [8] K. Nakamura, K.H. Jacob, J.N. Davies, Volcanoes as possible indicators of tectonic stress orientation; Aleutians and Alaska, *Pure Appl. Geophys.* 115 (1977) 87–112.
- [9] D.D. Pollard, O.H. Muller, D.R. Dockstader, The form and growth of fingered sheet intrusions, *Geol. Soc. Am. Bull.* 86 (1975) 351–363.
- [10] L. Geoffroy, J.P. Callot, C. Aubourg, M. Moreira, Magnetic and plagioclase linear fabric discrepancy in dykes: a new way to define the flow vector using magnetic foliation, *Terra Nova* 14 (2002) 183–190.
- [11] P.T. Delaney, D.D. Pollard, Deformation of host rocks and flow of magma during growth of minette dikes and breccia bearing intrusions near Ship Rock, New Mexico, *USGS Prof. Pap.* 1202 (1981) 61 pp.
- [12] K.L. Currie, J. Ferguson, The mechanism of intrusion of lamprophyre dikes indicated by 'offsetting' of dikes, *Tectonophysics* 9 (1970) 525–535.
- [13] Z. Reches, J. Fink, The mechanism of intrusion of the Inyo Dike, Long Valley Caldera, California, *J. Geophys. Res.* 93 (1988) 4321–4334.
- [14] G. Baer, Z. Reches, Flow patterns of magma in dikes, Makhtesh Ramon, Israel, *Geology* 15 (1987) 569–572.
- [15] G. Baer, Fracture propagation and magma flow in segmented dykes: field evidence and fabric analyses, Makhtesh, Israel, in: G. Baer, A. Heimann (Eds.), *Physics and Chemistry of Dykes*, A.A. Balkema, Rotterdam, 1995, pp. 125–140.
- [16] D. Shelley, Radial dikes of Lyttelton Volcano – their structure, form, and petrography, *NZ J. Geol. Geophys.* 31 (1988) 65–75.
- [17] A.R. Philpotts, P.M. Asher, Magmatic flow-direction indicators in a giant diabase feeder dike, Connecticut, *Geology* 22 (1994) 363–366.
- [18] M.D. Knight, G.P.L. Walker, Magma flow directions in dikes of the Koolau Complex, Oahu, determined from magnetic fabric studies, *J. Geophys. Res.* 93 (1988) 4301–4319.
- [19] H. Staudigel, J. Gee, L. Tauxe, R.J. Varga, Shallow intrusive directions of sheeted dikes in the Troodos ophiolite: Anisotropy of magnetic susceptibility and structural data, *Geology* 20 (1992) 841–844.
- [20] W.P. Moats, Geometry and Emplacement of Silicic Dikes at Summer Coon Volcano, Rio Grande and Saguache Counties, Colorado, M.S. Thesis, Arizona State University, Tempe, AZ, 1990, unpublished.
- [21] P.W. Lipman, T.A. Steven, L.H. Mehnert, Volcanic history of the San Juan mountains, Colorado, as indicated by potassium-argon dating, *Geol. Soc. Am. Bull.* 81 (1970) 2329–2352.
- [22] F.V. Perry, G. Woldegabriel, G.A. Valentine, E.K. Desmarais, G. Heiken, M. Heizler, M. Yamakawa, K. Ume-

- da, High-level radioactive waste disposal and volcanic hazard in Japan: A natural analog study of Summer Coon volcano, Colorado, *Geol. Soc. Am. Abstr. Programs* 31 (1999) A478.
- [23] P.W. Lipman, *Geology of the Summer Coon volcanic center, eastern San Juan Mountains, Colorado*, *Colorado Sch. Mines Q.* 63 (1968) 211–236.
- [24] S.A. Mertzman, *The Summer Coon volcano, eastern San Juan mountains, Colorado*, in: H.L. James (Ed.), *San Luis Basin Guidebook*, New Mexico Geological Society, Socorro, NM, 1971, pp. 265–272.
- [25] F.V. Perry, G.A. Valentine, E.K. Desmarais, G. Wolde Gabriel, Probabilistic assessment of volcanic hazard to radioactive waste repositories in Japan: Intersection by a dike from a nearby composite volcano, *Geology* 29 (2001) 255–258.
- [26] D.D. Pollard, O.H. Muller, The effect of gradients in regional stress and magma pressure on the form of sheet intrusions in cross section, *J. Geophys. Res.* 81 (1976) 975–984.
- [27] D.D. Pollard, Elementary fracture mechanics applied to the structural interpretation of dykes, in: H.C. Halls, W.F. Fahrig (Eds.), *Mafic Dyke Swarms*, *Geol. Soc. Can. Spec. Pap.* 34 (1987) 5–24.
- [28] D. Tarling, F. Hrouda, *The Magnetic Anisotropy of Rocks*, Chapman and Hall, New York, 1993.
- [29] L. Tauxe, *Paleomagnetic Principles and Practice*, Kluwer Academic, Dordrecht, 1998.
- [30] K. Benn, B. Allard, Preferred mineral orientations related to magmatic flow in ophiolite layered gabbros, *J. Petrol.* 30 (1989) 925–946.
- [31] J.L. Bouchez, Granite is never isotropic: An introduction to AMS studies of granitic rocks, in: J.L. Bouchez, D.H.W. Hutton, W.E. Stephens (Eds.), *Granite: From Segregation of Melt to Emplacement Fabrics*, Kluwer Academic, Dordrecht, 1997, pp. 95–112.
- [32] P. Rochette, M. Jackson, C. Aubourg, Rock magnetism and the interpretation of anisotropy of magnetic susceptibility, *Rev. Geophys.* 30 (1992) 209–226.
- [33] R.B. Hargraves, D. Johnson, C.Y. Chan, Distribution anisotropy: the cause of AMS in igneous rocks?, *Geophys. Res. Lett.* 18 (1991) 2193–2196.
- [34] L. Tauxe, J.S. Gee, H. Staudigel, Flow directions in dikes from anisotropy of magnetic susceptibility data: The bootstrap way, *J. Geophys. Res.* 103 (1998) 17775–17790.
- [35] R.G. Scott, K. Benn, Peak-ring rim collapse accommodated by impact melt-filled transfer faults, Sudbury impact structure, Canada, *Geology* 29 (2001) 747–750.
- [36] L.C. Correa-Gomes, C.R. Souza Filho, C.J.F.N. Martins, E.P. Oliveira, Development of symmetrical and asymmetrical fabrics in sheet-like igneous bodies: the role of magma flow and wall-rock displacements in theoretical and natural cases, *J. Struct. Geol.* 23 (2001) 1415–1428.
- [37] P. Rochette, C. Aubourg, M. Perrin, Is this magnetic fabric normal? A review and case studies in volcanic formations, *Tectonophysics* 307 (1999) 219–234.
- [38] C. Aubourg, G. Giordano, M. Mattei, F. Speranza, Magma flow in sub-aqueous rhyolitic dikes inferred from magnetic fabric analysis (Ponza Island, W. Italy), *Phys. Chem. Earth* 27 (2002) 1263–1272.
- [39] P. Rochette, L. Jenatton, C. Dupuy, F. Boudier, I. Reuber, Diabase dikes emplacement in the Oman Ophiolite: A magnetic fabric study with reference to geochemistry, in: T. Peters, A. Nicolas, R.G. Coleman (Eds.), *Ophiolite Genesis and Evolution of the Oceanic Lithosphere, Petrology and Structural Geology* 5, Kluwer Academic, London, 1991, pp. 55–82.
- [40] L. Tauxe, C. Constable, L. Stokking, C. Badgley, Use of anisotropy to determine the origin of characteristic remanence in the Siwalik Red Beds of northern Pakistan, *J. Geophys. Res.* 95 (1990) 4391–4404.
- [41] M.A. Khan, The anisotropy of magnetic susceptibility of some igneous and metamorphic rocks, *J. Geophys. Res.* 67 (1962) 2873–2885.
- [42] B.B. Ellwood, Flow and emplacement direction determined for selected basaltic bodies using magnetic susceptibility anisotropy measurements, *Earth Planet. Sci. Lett.* 41 (1978) 254–264.
- [43] D. Liss, D.H.W. Hutton, W.H. Owens, Ropy flow structures: A neglected indicator of magma-flow direction in sills and dikes, *Geology* 30 (2002) 715–718.
- [44] J.-P. Callot, L. Geoffroy, C. Aubourg, J.P. Pozzi, D. Mege, Magma flow directions of shallow dikes from the East Greenland volcanic margin inferred from magnetic fabric studies, *Tectonophysics* 335 (2001) 313–329.
- [45] R.J. Varga, J.S. Gee, H. Staudigel, L. Tauxe, Dike surface lineations as magma flow indicators within the sheeted dike complex of the Troodos Ophiolite, Cyprus, *J. Geophys. Res.* 103 (1998) 5241–5256.
- [46] D. Shelley, Determining paleo-flow directions from groundmass fabrics in the Lyttelton radial dykes, New Zealand, *J. Volcanol. Geotherm. Res.* 25 (1985) 69–79.
- [47] P. Launeau, A.R. Cruden, J.-L. Bouchez, Mineral recognition in digital images of rocks: a new approach using multichannel classification, *Can. Mineral.* 32 (1994) 919–933.
- [48] P. Launeau, P.-Y.F. Robin, Fabric analysis using the intercept method, *Tectonophysics* 267 (1996) 91–119.
- [49] G. Baer, Mechanisms of dike propagation in layered rocks and in massive, porous sedimentary rocks, *J. Geophys. Res.* 96 (1991) 11911–11929.
- [50] A. Gudmundsson, Formation of dykes, feeder-dykes, and the intrusion of dykes from magma chambers, *Bull. Volcanol.* 47 (1984) 537–550.
- [51] J.E. Olson, D.D. Pollard, The initiation and growth of en echelon veins, *J. Struct. Geol.* 13 (1991) 595–608.
- [52] P.T. Delaney, D.D. Pollard, J.I. Ziony, E.H. McKee, Field relations between dikes and joints; emplacement processes and paleostress analysis, *J. Geophys. Res.* 91 (1986) 4920–4938.